

Sizzled Is Unique among Secreted Frizzled-related Proteins for Its Ability to Specifically Inhibit Bone Morphogenetic Protein-1 (BMP-1)/Tolloid-like Proteinases^{*[5]}

Received for publication, May 11, 2012, and in revised form, July 3, 2012. Published, JBC Papers in Press, July 23, 2012, DOI 10.1074/jbc.M112.380816

Cécile Bijakowski[‡], Sandrine Vadon-Le Goff[‡], Frédéric Delolme[‡], Jean-Marie Bourhis^{#1}, Pascaline Lécorché[§], Florence Ruggiero[¶], Christoph Becker-Pauly^{||}, Irene Yiallourou^{**}, Walter Stöcker^{**}, Vincent Dive[§], David J. S. Hulmes[‡], and Catherine Moali^{‡2}

From the [‡]Institut de Biologie et Chimie des Protéines, CNRS/Université de Lyon FRE3310/FR3302, 69367 Lyon cedex 7, France, [§]CEA Saclay, SIMOPRO, 91191 Gif-sur-Yvette, France, [¶]Institut de Génomique fonctionnelle de Lyon, ENS de Lyon/CNRS UMR 5242, 69364 Lyon cedex 7, France, ^{||}Institute of Biochemistry, Unit for Degradomics of the Protease Web, Christian-Albrechts-University, 24118 Kiel, Germany, and the ^{**}Institute of Zoology, Cell and Matrix Biology, Johannes Gutenberg-University, 55128 Mainz, Germany

Background: *Xenopus* and zebrafish BMP-1/tolloid-like proteinases (BTPs) are inhibited by sizzled, a secreted frizzled-related protein (sFRP) not present in mammals.

Results: *Xenopus* sizzled is a very potent inhibitor of human BTPs, whereas mammalian sFRPs have no effect.

Conclusion: Regulation of BTP activity by sFRPs is not conserved in mammals.

Significance: Sizzled is the most potent exogenous inhibitor of human BTPs.

BMP-1/tolloid-like proteinases (BTPs) are major enzymes involved in extracellular matrix assembly and activation of bioactive molecules, both growth factors and anti-angiogenic molecules. Although the control of BTP activity by several enhancing molecules is well established, the possibility that regulation also occurs through endogenous inhibitors is still debated. Secreted frizzled-related proteins (sFRPs) have been studied as possible candidates, with highly contradictory results, after the demonstration that sizzled, a sFRP found in *Xenopus* and zebrafish, was a potent inhibitor of *Xenopus* and zebrafish tolloid-like proteases. In this study, we demonstrate that mammalian sFRP-1, -2, and -4 do not modify human BMP-1 activity on several of its known substrates including procollagen I, procollagen III, pN-collagen V, and prolyl oxidase. In contrast, *Xenopus* sizzled appears as a tight binding inhibitor of human BMP-1, with a K_i of 1.5 ± 0.5 nM, and is shown to strongly inhibit other human tolloid isoforms mTLD and mTLL-1. Because sizzled is the most potent inhibitor of human tolloid-like proteinases known to date, we have studied its mechanism of action in detail and shown that the frizzled domain of sizzled is both necessary and sufficient for inhibitory activity and that it acts directly on the catalytic domain of BMP-1. Residues in sizzled required for inhibition include Asp-92, which is shared by sFRP-1 and -2, and also Phe-94, Ser-43, and Glu-44, which are

specific to sizzled, thereby providing a rational basis for the absence of inhibitory activity of human sFRPs.

Bone morphogenetic protein-1 (BMP-1)³ is the prototype of a small group of zinc metalloproteinases, the BMP-1/tolloid-like proteinases (BTPs), which include members in species ranging from *Drosophila* to human (1). In mammals, there are four isoforms of BTPs (supplemental Fig. S1): BMP-1 and mTLD (mammalian tolloid), which are alternative spliced products of the same gene (2), and also mTLL-1 and mTLL-2 (mammalian tolloid-like 1 and 2) (3, 4). These proteinases are characterized by a highly similar domain structure encompassing a signal peptide, a propeptide that maintains latency of the enzyme (5), a catalytic domain belonging to the astacin subfamily (M12A according to MEROPS database) (6), and a variable number of CUB (Complement, Uegf, BMP-1) and epidermal growth factor (EGF) auxiliary domains. Other members of the astacin subfamily in humans include meprins α and β and ovas-tacin (supplemental Fig. S1). BTPs have been found to be active on more than 20 substrates, including components of the extracellular matrix, growth factors, and pro/anti-angiogenic factors and are thought to play major roles in development (7), tissue repair, and related pathological conditions such as fibrosis (8, 9).

An interesting feature of the BTPs is the fact that their regulation seems to rely mainly on specific enhancers which can direct activity toward distinct subsets of substrates (10). For

* This work was supported by the Agence Nationale de la Recherche (projects SCAR FREE and TOLLREG), the Fondation de France, the CNRS, the Université Claude Bernard Lyon 1, the Lyon Biopôle (to D. J. S. H. and C. M.), Deutsche Forschungsgemeinschaft Grants Sto185/3–2, SFB492 (to W. S. and I. Y.), BE 4086/1–2, SFB877, and the Cluster of Excellence “Inflammation at Interfaces” (to C. B.-P.).

[5] This article contains supplemental Tables S1 and S2 and Figs. S1–S5.

¹ Present address: Université Joseph Fourier/European Molecular Biology Laboratory/CNRS UMI3265, 38042 Grenoble cedex 9, France.

² To whom correspondence should be addressed: Institut de Biologie et Chimie des Protéines, CNRS/Université de Lyon FRE3310, 7 Passage du Vercors, 69367 Lyon cedex 7, France. Tel.: 33-4-72-72-26-38; Fax: 33-4-72-72-26-04; E-mail: c.moali@ibcp.fr.

³ The abbreviations used are: BMP-1, bone morphogenetic protein-1; BTP, BMP-1/tolloid-like proteinase; CUB, Complement, Uegf, BMP-1; Dnp, 2,4-dinitrophenyl; Dpa, N-(2,4-dinitrophenyl)-L-diaminopropionyl; Mca, (7-methoxycoumarin-4-yl)acetyl; Fz, frizzled; mTLD, mammalian tolloid; mTLL-1, mammalian tolloid-like 1; mTLL-2, mammalian tolloid-like 2; MMP, matrix metalloproteinase; PCPE, procollagen C-proteinase enhancer; sFRP, secreted frizzled-related protein; TIMP, tissue inhibitor of matrix metalloproteinase; NTR, netrin-like.

Control of BTP Activity by sFRPs

example, procollagen C-proteinase enhancers (PCPEs) enhance the cleavage of fibrillar procollagens (11–13), whereas twisted gastrulation and ONT-1 (Olfactomedin Noelin Tiarin factor 1) are both activators of chordin cleavage (14, 15), and periostin enhances the maturation of prolyl oxidase (16). However, it is not always known if these effects are achieved through direct or indirect mechanisms. In contrast to other extracellular metalloproteinases of the metzincin family like matrix metalloproteinases (MMPs; supplemental Fig. S1) for which well established specific endogenous inhibitors have been described (e.g. TIMPs, tissue inhibitors of matrix metalloproteinases), the data concerning specific endogenous inhibitors of human BTPs are presently limited and controversial. In 2009, Lee *et al.* (17) showed that BMP-4, a member of the transforming growth factor- β superfamily, inhibits BTPs in a non-competitive manner by binding to their CUB domains. However, this result is questioned by a previous study showing that mature BMP-1 is unable to interact with BMP-4 (18). Equally controversial is the potential role of secreted frizzled-related proteins (sFRPs) in the regulation of BTP activity.

The family of sFRPs includes five members in mammals (sFRP-1 to sFRP-5) and additional members in some species of vertebrates (sizzled, crescent, and Tlc). They are characterized by the presence of two domains, a netrin-like (NTR) domain, homologous to the N-terminal domain of TIMPs and to the C-terminal domain of PCPEs, and a frizzled (Fz) domain structurally related to the extracellular Wnt binding domain of frizzled receptors. Due to this homology, sFRPs have been mainly studied for their role as antagonists of Wnt signaling. However, recent studies have shown that sFRPs are not only Wnt-binding proteins but have a wide range of biological activities (19). In support of this idea was the finding that sizzled is an inhibitor of *Xenopus* and zebrafish BTPs (20, 21).

Sizzled was initially identified in *Xenopus* embryos as a putative Wnt8 antagonist (22), but subsequent studies showed that sizzled was unable to block Wnt signaling *in vivo* (23–25). Rather, sizzled was shown to inhibit BMP signaling, thereby playing an important role in dorso-ventral patterning of *Xenopus* and zebrafish embryos (24–26). It does this by inhibiting BTPs and thus stabilizing chordin, which is both a BMP antagonist and a BTP substrate. Further biochemical studies suggested that the Fz domain of sizzled binds and competitively inhibits non-mammalian BTPs (20, 21). More recently, *Xenopus* crescent, which is the closest relative of sizzled, was also shown to inhibit BTPs (27) but remains capable of interfering with Wnt signaling. These findings reveal a new role for sFRPs as inhibitors of BTPs, but because sizzled and crescent genes are not present in mammals, this raises the question of whether or not this mechanism of inhibition is conserved in this class of vertebrates.

In recent years much attention has been paid to mouse sFRP-2 and its activity on *Xenopus* and human BTPs. Although it was shown to potentially inhibit *Xenopus* Xlr in the initial study by Lee *et al.* (20), Kobayashi *et al.* (9) reported a few years later that, far from inhibiting human BMP-1, sFRP-2 was a specific enhancer of procollagen I cleavage and that this enhancement could promote fibrosis in a rat model of infarcted heart. In contrast, He *et al.* (28) showed that high concentrations of sFRP-2

inhibited the cleavage of a fluorogenic peptide and of procollagen I by human BMP-1, and using a similar model, they concluded that direct injection of sFRP-2 in the infarcted heart could inhibit fibrosis and improve cardiac function. Finally, a third study from von Marschall *et al.* (29) found that sFRP-2 had no effect on the procollagen-C-proteinase activity of BMP-1.

Given the apparent conflict between the data, it appeared necessary to carefully re-evaluate whether the inhibition of BTPs is a general property of all sFRPs. In this study, we used five different substrates of human BMP-1 to check if its activity was inhibited or activated by three mammalian sFRPs (sFRP-1, sFRP-2, and sFRP-4). All tests led to the same conclusion that none of the tested sFRPs is able to enhance or inhibit BMP-1 activity in the conditions used for the activity assays. In contrast, *Xenopus* sizzled proved to be a selective and potent inhibitor of human BMP-1, with an inhibition constant in the low nanomolar range. Based on the sequence differences between sizzled and sFRP-1 and -2, its closest human relatives, we used site-directed mutagenesis to map the first interaction surface for sizzled and thus propose a model for the mechanism of inhibition of BMP-1.

EXPERIMENTAL PROCEDURES

Materials—Recombinant human Wnt3a, mouse sFRP-2, human sFRP-4, and full-length human MMP-1, -8, and -13 were obtained from R&D Systems. Human sFRP-1 was either from R&D Systems or produced as described below. All other proteins were produced and expressed as described below.

Molecular Biology—The cDNA for *Xenopus laevis* sizzled in the pCS2+ plasmid (gift from E.M. De Robertis, Los Angeles, CA) was amplified by PCR and inserted in-frame with a C-terminal V5-His₆ tag in the pcDNA3.1/V5-His-TOPO vector (Invitrogen). *Pfx* platinum polymerase (Invitrogen) was used for the PCR reaction, and the primers were as follows (the sequence used to insert a thrombin cleavage site between the sequence of sizzled and the V5-His₆ tag is underlined): 5'-GAACATGTCCGGAGTCTTCCTGCT-3' and 5'-ACTACCGCGTGGCACCAGACATTTATGATGTCTCCACCTCCTTG-3'. The cDNA for sizzled in-frame with the V5-His₆ tag was then excised with KpnI/PmeI and subcloned into the pCEP4 vector (Invitrogen) digested with KpnI/NaeI. The cDNA for human sFRP-1 in the pBlueScriptR plasmid (ImaGenes) was subcloned into pcDNA3.1/V5-His-TOPO and pCEP4 vectors using the same strategy with the following primers: 5'-GGCATGGGCATCGGGCGCAGCG-3' and 5'-ACTACCGCGTGGCACCAGCTTAAACACGGACTGAAGGTGGG-3'.

All mutations and deletions were generated with the QuikChange XL site-directed mutagenesis kit from Stratagene. The coding sequences for sizzled and sFRP-1 in pCEP4 were used as templates to generate the mutants sizzled-C115S/C159S, sizzled-D92N, sizzled-F94A, sizzled-Q96A, sizzled-K26A, sizzled-S43A/E44A, and sFRP-1-R124T/P125F/Y127Q. These mutants were obtained using overlapping primers with mutated bases in the middle and melting temperatures above 78 °C. The coding sequence for sizzled-C115S/C159S in pCEP4 was also used as a template to generate individual Fz and NTR

domains. 5'-Phosphorylated primers were designed to delete residues 138–281 to obtain Fz (numbering includes the signal peptide) and residues 19–137 to obtain NTR. The 5'-phosphorylated PCR products were then ligated with T4 DNA ligase (rapid DNA ligation kit, Fermentas). Similarly, the coding sequence for sFRP-1 in pCEP4 was used as a template to obtain the constructs sFRP-1-Fz (deleted residues 171–314) and sFRP-1- Δ Nterm (deleted residues 32–52).

Protein Production and Purification— ^3H Procollagen I was prepared from the medium of freshly isolated chick embryo fibroblasts incubated with ^3H tryptophan as described (30). All other proteins used were recombinant. Human procollagen III (12), prolyl oxidase (12), pN-collagen V homotrimer (31), BMP-1-FLAG (32), and mTLL-1 (with a C-terminal His₆ tag; cDNA a gift from Dr. E. Canty, University of Liverpool) (33) were produced in 293-EBNA cells and purified as previously described. Similarly, human mTLD (cDNA a gift from Prof. A. Sieron, Medical University of Silesia, Katowice, Poland) was produced in 293-EBNA cells and purified like untagged BMP-1 (12).

Sizzled, sFRP-1, and their mutants were also produced in 293-EBNA cells after transfection with the pCEP4 constructs described in the previous section using Lipofectamine (Invitrogen) as the transfection agent. After 24 h, hygromycin B (300 $\mu\text{g}/\text{ml}$) was added to the medium, and selection was maintained for the duration of cell amplification. Protein production was performed in Cellstack culture chambers (Corning) using Dulbecco's modified Eagle's medium (PAA) containing 50 $\mu\text{g}/\text{ml}$ gentamycin. Medium was collected every 2 days and stored at -80°C . Pooled medium was then centrifuged to remove cell debris and incubated with nickel nitrilotriacetic acid-agarose (Qiagen, 15 ml/liter) for 3 h at 4°C . The resin was then packed into a column, rinsed with 50 mM imidazole in 50 mM NaH_2PO_4 , 0.3 M NaCl, pH 8, and His-tagged proteins were eluted with 250 mM imidazole in the same buffer. Pooled fractions were concentrated using Amicon Ultra centrifugal filter devices (Millipore), and imidazole was removed using PD-10 desalting columns (GE Healthcare) according to the manufacturer's instructions. Human soluble meprins α and β were produced in insect cells, purified by streptactin or Ni-NTA chromatography, and trypsin-activated as described (34, 35). BMP-1cat (36) and recombinant astacin (37, 38) were expressed in *Escherichia coli*, purified, and re-folded as reported. The catalytic domains of MMP-9 and -12 were produced as described (39, 40).

Circular Dichroism—Far UV (180–260 nm) CD measurements were carried out using thermostated 0.2-mm path length quartz cells in an Applied Photophysics Chirascan instrument (Plateau Production et Analyse des Protéines; UMS 3444). Proteins (0.1–0.5 mg/ml) were analyzed at 25°C in 20 mM Tris- H_2SO_4 , 0.15 M NaF, pH 7.4. Spectra were measured with a wavelength increment of 0.5 nm, integration time of 6 s, and bandpass of 1 nm. Protein concentrations were determined by the Bradford assay.

Mass Spectrometry—Sizzled was digested with sequencing grade trypsin (Promega; 20/1, protein/enzyme) for 1 h at 50°C with continuous stirring without reduction/alkylation. Liquid chromatography-mass spectrometry (LC-MS) experiments

were performed at the Centre Commun de Microanalyse des Protéines of UMS3444 on a LTQ Velos mass spectrometer (Thermo Scientific) equipped with an Ultimate 3000 nanoLC pump (Dionex). A C_4 column (Dionex, 75- μm inner diameter \times 15 cm, 300 \AA pore, and 5- μm particle size) was coupled online to the mass spectrometer through a nanospray needle (New Objective). A 20-min linear gradient was applied using mobile phase A (0.1% formic acid and 10% acetonitrile in water) and mobile phase B (0.1% formic acid and 80% acetonitrile in water) at 300 nl/min. The mass spectrometer was operated in MS mode only using zoom scan.

Activity Assays—BMP-1 activity in the presence of its substrates ^3H procollagen I, procollagen III, pN-collagen V, prolyl oxidase, and mini-procollagen III was measured as previously described (12) at 37°C in 50 mM HEPES, 0.15 M NaCl, 5 mM CaCl_2 , 0.02% Brij, pH 7.4 (buffer A) with incubation times and protein concentrations as indicated. Cleavage of mini-procollagen III by mTLD, mTLL-1, and meprins (41) was analyzed like cleavage by BMP-1 in buffer A at 37°C .

Activities of BMP-1 (20–36 nM), BMP-1cat (1 μM), astacin (89 nM), meprin α (1.9 nM), and meprin β (0.8 nM) were analyzed using the quenched fluorescent peptide Mca-YVADAP-K(Dnp)-OH (Bachem). The reactions were carried out in black low-binding microtiter plates using 10–40 μM peptide and 10–1000 nM potential inhibitor in 50 mM HEPES, 0.15 M NaCl, 5 mM CaCl_2 , 0.02% *n*-octyl- β -D-glucopyranoside, 2% DMSO, pH 7.4 (final volume 100 μl). After preincubation for 10 min at 37°C , the reaction was started by the addition of enzyme, and subsequent changes in fluorescence were monitored at 405 nm (excitation at 330 nm) in a TECAN spectrofluorimeter for 20 min. Similarly, the activity of recombinant MMPs was assayed at 400 nm with a Fluoroskan Ascent photoncounter spectrophotometer (ThermoLab Systems) using 9 μM fluorogenic synthetic substrate Mca-PLGL(Dpa)AR-NH₂ (Enzo; excitation, 340 nm) in 50 mM HEPES, 0.15 M NaCl, 5 mM CaCl_2 , 0.02% *n*-octyl- β -D-glucopyranoside, 0.5% DMSO, pH 7.4, at room temperature. Sizzled (from 10–474 nM) was preincubated with MMP for 30 min before substrate addition.

Surface Plasmon Resonance—The interaction between sizzled and BMP-1 was studied by surface plasmon resonance experiments using a Biacore T100 instrument (Plateau Production et Analyse des Protéines; UMS 3444). Sizzled was immobilized in 10 mM HEPES, 0.15 M NaCl, pH 7.4, on a CM5 sensorchip (series S) using amine coupling chemistry. The control channel was prepared with the same activation/deactivation procedure except that the protein solution was replaced by buffer alone. Before injection, analyte buffer was exchanged with 10 mM HEPES, 0.15 M NaCl, 5 mM CaCl_2 , 0.05% P-20, pH 7.4, using a Zeba Desalt Spin Column (Thermo Scientific). The same buffer was used as running buffer, and sensorgrams were recorded at 25°C with a flow rate of 30 $\mu\text{l}/\text{min}$. Regeneration of active and control channels was performed using 2 M guanidinium chloride. Other surface plasmon resonance experiments were performed in a similar manner except that a different running buffer was used in experiments involving Wnt3a (10 mM HEPES, pH 7.4, 0.15 M NaCl, 3 μM EDTA, 0.05% P-20, 1% CHAPS). Also, immobilization of BMP-1 or the anti-His antibody (R&D Systems) was performed at pH 4.5 (in 10 mM

Control of BTP Activity by sFRPs

sodium acetate buffer), and corresponding interactions were regenerated with different solutions (50% ethylene glycol then 2 M NaCl for interactions involving BMP-1, 10 mM glycine, pH 2, to release sizzled captured on the anti-His antibody). Kinetic data were analyzed using Biacore T100 Evaluation software 2.0.2.

Molecular Modeling—The model for the Fz domain of sizzled was obtained by comparative homology modeling using the crystal structures of the cysteine-rich domain of secreted frizzled related protein 3 (PDB code 1IJX) and of the cysteine-rich domain of mouse frizzled 8 (PDB code 1IJY) as templates (with a sequence identity of 35 and 32%, respectively) (42). Sequences were aligned using MAFFT with manual adjustments. Based on this multiple alignment, the program Modeler (43) was used to generate a three-dimensional representation of the Fz domain (from residues 26 to 136 of sizzled). The loop between residues 91 and 97 was subjected to several rounds of refinement as implemented in Modeler (43). The geometry of the final model was checked with MolProbity (44).

RESULTS

Sizzled, but Not Mammalian sFRPs, Can Inhibit Human BMP-1—To evaluate which human sFRP is the most likely to inhibit human BMP-1, we compared their Fz domains with the Fz domain of sizzled (Fig. 1A). For sFRP-1, sFRP-2, and sFRP-5, the percentage of sequence identity is around 50 (50, 47.2, and 47%, respectively), whereas it is only around 30% for sFRP-3 and sFRP-4 (32.2 and 29%, respectively). We decided to analyze the effect on BMP-1 activity of one member of each subgroup, namely sFRP-1 and sFRP-4, as well as of sFRP-2 for which the largest amount of data is available. As most regulators of BTPs are substrate-specific (10, 12, 14–16, 45), it seemed important to test the effect of sFRPs on the cleavage of several substrates.

The first substrates to be tested were the fibrillar procollagens I and III for which removal of C-propeptide by BTPs is necessary for incorporation into fibrils (46). First, the conversion of [³H]procollagen I to pN-collagen I and C-propeptide was monitored by a quantitative assay based on the detection of the radioactivity emitted by the soluble C-propeptide after precipitation of procollagen and pN-collagen (12, 47). In this assay human sFRP-1, mouse sFRP-2, and human sFRP-4 (100 nM) had no effect on BMP-1 activity, whereas the same concentration of sizzled from *X. laevis* led to a decrease in BMP-1 activity to $23 \pm 7\%$ of its initial value (Fig. 2A). A previous study reported that low concentrations of sFRP-2 (10–20 nM) could enhance the cleavage of procollagen I by BMP-1, whereas higher concentrations (100–200 nM) led to inhibition (28). To check for a possible concentration-dependent effect, we analyzed the cleavage of procollagen I in the presence of increasing concentrations of sFRP-2 (10, 50, 200, and 1000 nM) in conditions leading to 45% processing of the substrate by BMP-1. In our hands, however, sFRP-2 was still unable to inhibit or enhance BMP-1 activity (supplemental Fig. S2A) throughout this concentration range. Similarly, the processing of procollagen III into pN-collagen III was unaffected by mammalian sFRPs but was inhibited by sizzled (Fig. 2B). To eliminate the possibility that the lack of activity of recombinant sFRP-1 and -2 was due to denaturation or aggregation of these proteins, we

checked their ability to interact with Wnt3a, one of their well known ligands (48), by surface plasmon resonance. As shown in supplemental Fig. S3A, human Wnt3a interacted well with both sFRPs when the latter were immobilized on a sensorchip.

Another substrate of BMP-1 is procollagen V, which regulates the size of collagen I fibrils. In contrast to procollagens I and III, BMP-1 processing can occur in both the N- and C-propeptide regions of procollagen V (49–52). Here we have used the pN-collagen form of the procollagen $\alpha 1(V)$ homotrimer, which is converted by BMP-1 to mature collagen by release of the N-propeptide. Only sizzled was able to inhibit this conversion, as can be seen by the decreased intensity of the band corresponding to the N-propeptide (Fig. 2C). The last physiological substrate to be tested was prolyl oxidase, whose mature form is responsible for the stabilization of collagen and elastin networks through the initiation of the formation of covalent cross-links (53). As shown in Fig. 2D, the addition of BMP-1 led to an increase in intensity of the band corresponding to mature lysyl oxidase, which could be prevented only by sizzled.

In addition to these physiological substrates, we also tested the ability of sFRPs to inhibit the cleavage of mini-procollagen III, a model substrate derived from procollagen III (which consists of the C-propeptide, the C-telopeptide, and a very short triple helix made of the last 33 triplets of procollagen III (12)) and of the fluorogenic peptide Mca-YVADAPK(Dpn)-OH, originally described for caspases (20, 54). In the presence of 100 nM sizzled, the residual activity of BMP-1 was only $4 \pm 3\%$ that of the control activity with mini-procollagen III (Fig. 2E) and $27 \pm 3\%$ that of the control activity with the fluorogenic peptide (Fig. 2F). As for sFRP-1, sFRP-2, and sFRP-4, these proteins neither inhibited nor enhanced BMP-1 activity with these substrates. Because other authors may have used slightly different buffer conditions, we checked whether small variations of pH (between 7.0 and 8.0), HEPES concentration (10–200 mM), calcium concentration (0–50 mM), or replacement of HEPES buffer by Tris might modify any effects of sFRP-2 on cleavage of mini-procollagen III by BMP-1 but found no differences (data not shown).

Finally, we tested the possibility that sizzled and the three sFRPs of interest could be substrates of BMP-1, but none of them was found to yield detectable cleavage products by SDS-PAGE when incubated for 3 h at 37 °C in the presence of 100 nM BMP-1 (data not shown). Neither were they cleaved by the two other main human astacin-like proteases, meprins α and β (55), which were recently demonstrated to have procollagen C-proteinase activity (41). Because one report suggested that sFRP-2 selectively targets this activity of the BMP-1/tolloid-like proteinases (9), we also verified that cleavage of mini-procollagen III by meprins was not affected by sFRP-1 and sFRP-2 (supplemental Fig. S2B).

Altogether, these studies indicate that sFRP-1, sFRP-2, and sFRP-4 are neither inhibitors, nor enhancers, nor substrates of human BMP-1, at least in our conditions. In contrast, it appears that *Xenopus* sizzled is an inhibitor not only of *Xenopus* BTPs but also of human BMP-1.

Sizzled Is a Potent Inhibitor of Human BMP-1—We next performed a kinetic analysis to determine the inhibition constant (K_i) for sizzled on BMP-1. For this purpose we used the fluoro-

Control of BTP Activity by sFRPs

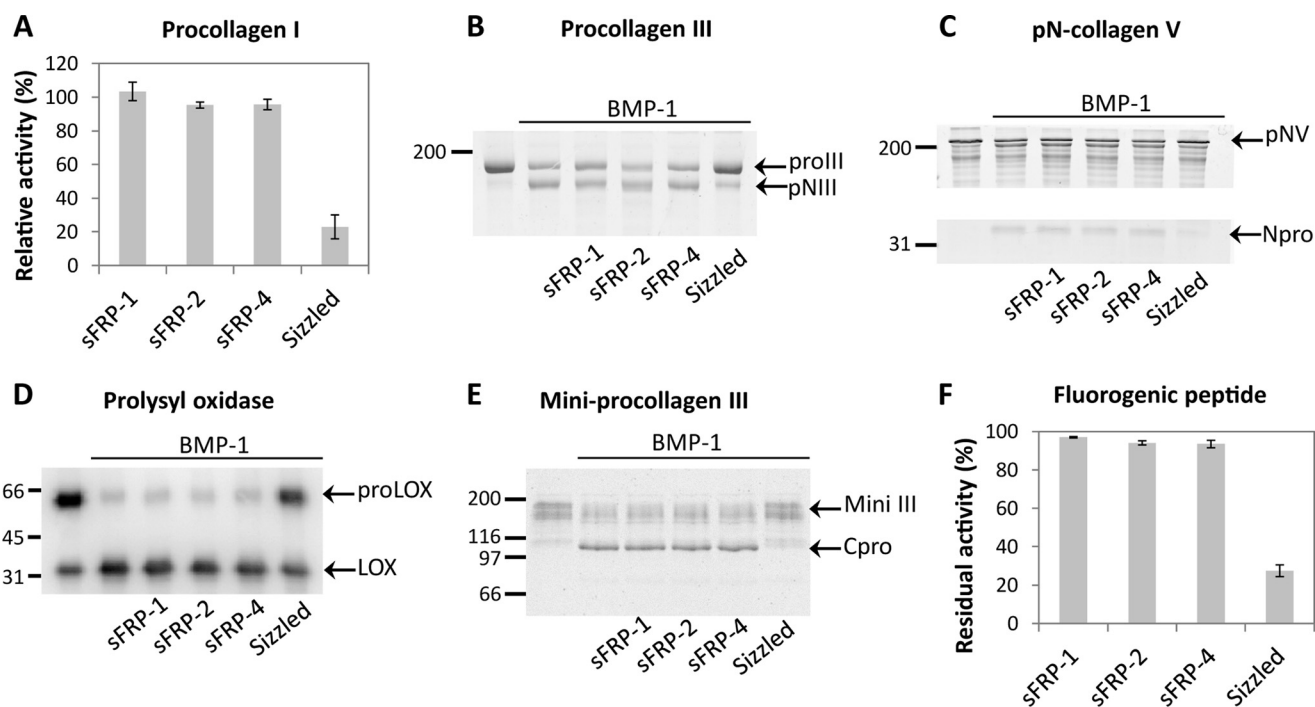


FIGURE 2. Effect of sizzled, sFRP-1, -2, and -4 on BMP-1 activity. The following substrates were incubated at 37 °C with or without BMP-1 in the presence or in the absence of 100 nM human sFRP-1, mouse sFRP-2, human sFRP-4, or *Xenopus* sizzled. **A**, [³H]procollagen I (360 nM) was incubated with BMP-1 (18 nM) for 100 min. Activities are expressed relative to activity in the absence of any sFRP (Means ± S.D., *n* = 3). **B**, procollagen III (44 nM) was incubated with BMP-1 (23 nM) for 3 h, and the products were analyzed by SDS-PAGE (6% acrylamide in the separating gel, reducing conditions) followed by staining with EZ Blue. **C**, partially purified pN-collagen V homotrimer was incubated with BMP-1 (48 nM) for 6 h, and release of the N-propeptide was analyzed by SDS-PAGE (10% acrylamide, reducing conditions) followed by staining with EZ Blue. **D**, prolyl oxidase was incubated with BMP-1 (19 nM) for 2 h. Analysis was by SDS-PAGE (10% acrylamide, reducing conditions) followed by Western blotting with an anti-V5 antibody (Invitrogen). **E**, mini-procollagen III (330 nM) was incubated with BMP-1 (16 nM) for 1.5 h, and the products were analyzed by SDS-PAGE (8% acrylamide, non-reducing conditions) followed by staining with SYPRO Ruby (Sigma) and detection/quantification on a Storm 860 Imager. **F**, the fluorogenic quenched peptide (20 μM) was incubated with BMP-1 (21 nM), and the fluorescence emitted by the products was monitored for 20 min. Activities are expressed relative non-reducing to activity in the absence of any sFRP and correspond to the means ± S.D. (*n* = 4).

We also studied the interaction between sizzled and BMP-1 by surface plasmon resonance. As shown in supplemental Fig. S3B, BMP-1 was found to bind immobilized sizzled in a concentration-dependent manner. Incidentally, the interaction was found to be reversible and could be regenerated with 2 M guanidinium chloride. The curves were best fitted with the “heterogeneous ligand” model, assuming that there are two binding sites for BMP-1 on sizzled, and the two calculated dissociation constants (K_D) were 6.0 nM (accounting for 58% of the signal) and 37 nM (accounting for 42% of the signal). This heterogeneity was induced by the coupling procedure as it disappeared when sizzled was captured with an anti-His antibody, leading to a single K_D of 14 nM (by single-cycle analysis; Fig. 3B). In addition, the fast on-rate of the BMP-1/sizzled interaction ($2.5 \times 10^5 \text{ M}^{-1} \text{ s}^{-1}$) together with the absence of effect of enzyme preincubation with inhibitor in activity assays (data not shown) indicate that sizzled does not behave as a “slow-binding” inhibitor.

These two complementary approaches both showed that sizzled strongly binds and inhibits human BMP-1 in a reversible manner with an inhibition constant in the nanomolar range. More unexpectedly, when the interaction of BMP-1 with sFRP-1, -2, and -4 was tested by surface plasmon resonance (supplemental Fig. S3C), we found that sFRP-1 and -2, but not sFRP-4, were also able to bind BMP-1.

Sizzled Is a Specific Inhibitor of BTPs—We next investigated if sizzled was able to inhibit two other human BTPs: mTLD and mTLL-1. These proteinases were also able to cleave mini-procollagen III. In the presence of increasing concentrations of sizzled, mTLD and mTLL-1 were both inhibited to the same extent as BMP-1 (Fig. 4A). Then, the effect of sizzled was tested on other members of the astacin family, including crayfish astacin, the founder member of the family, and human meprins α and β (6). Using the fluorogenic peptide substrate, we found no evidence of inhibition of crayfish astacin, meprin α , nor meprin β by sizzled, even at a concentration of 1 μM (Fig. 4B). This result was confirmed for meprins on the mini-procollagen III substrate with 100 nM sizzled (supplemental Fig. S2B). The remarkably high specificity of sizzled was also shown with a panel of five representative MMPs (MMP-1, MMP-8, MMP-9, MMP-12, and MMP-13), which were found to be essentially unaffected by sizzled at concentrations more than 100 times greater than the K_i found for BMP-1 (Fig. 4C). We conclude that sizzled is a potent and specific inhibitor of BTPs.

Sizzled Inhibits the Catalytic Domain of BMP-1 by Its Fz Domain—According to their finding that sizzled inhibited *Xenopus* BTPs in a competitive manner, Lee *et al.* (20) suggested that sizzled bound the catalytic domains of these enzymes. In contrast to this proposal, Kobayashi *et al.* (9) showed data from pulldown assays indicating that sizzled

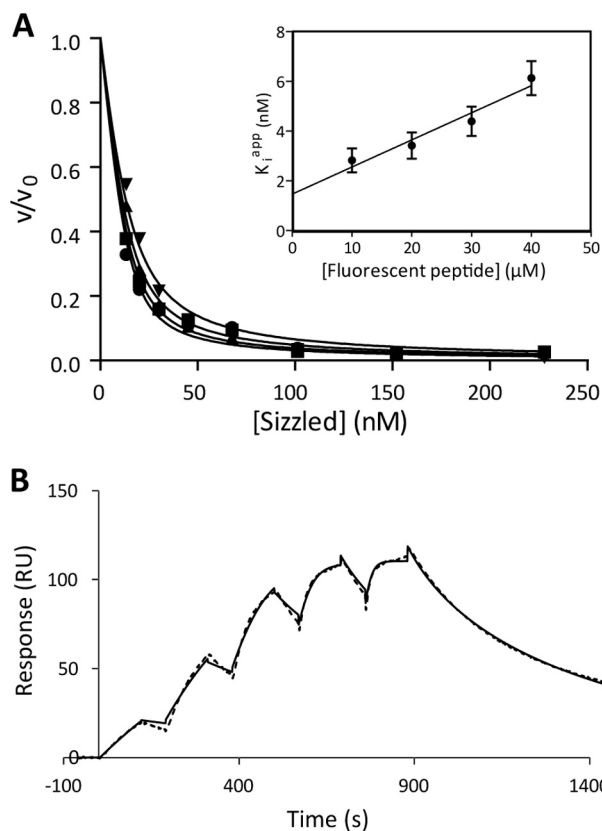


FIGURE 3. Sizzled is a potent inhibitor of human BMP-1. *A*, shown is a plot of fractional velocity as a function of sizzled concentration at different fluorescent peptide concentrations. Inhibition assays were conducted with the fluorescent peptide at 10 μM (\bullet), 20 μM (\blacksquare), 30 μM (\blacktriangle), and 40 μM (\blacktriangledown). BMP-1 concentration was 20 nM, and sizzled concentrations varied between 13.3 and 227.8 nM. *Solid lines* represent best fits obtained using the Morrison equation. The *inset* shows the secondary plot of K_i^{app} (\pm S.D.) as a function of fluorescent peptide concentration. The *y* intercept of this plot is the K_i value. Curves were fitted using GraphPad Prism 5. *B*, interaction of BMP-1 with sizzled was studied by surface plasmon resonance. The curves were obtained in "single cycle" mode by injecting increasing concentrations of BMP-1 (20, 40, 80, 160, and 320 nM) at a flow rate of 30 $\mu\text{l}/\text{min}$ for 120 s on captured sizzled (60 resonance units (RU) captured). *Dotted line* represents experimental curve, and fit with the "1:1 binding" model is shown as *solid line* ($\chi^2 = 2.80$).

bound BTPs through the non-catalytic domains. To further investigate this question and confirm our kinetic experiments suggesting a competitive inhibition, we tested the ability of sizzled to inhibit the catalytic domain of BMP-1 (BMP-1cat) produced in bacteria (36). Using the fluorogenic peptide as a substrate, a BMP-1cat concentration 27-fold higher than the concentration of BMP-1 was necessary to reach the same reaction rate. This observation can be explained either by the fact that the catalytic domain alone is less efficient than full-length BMP-1 in cleaving the peptide or by the fact that a fraction of BMP-1cat produced in bacteria is inactive. As shown in Fig. 5A, sizzled inhibited BMP-1cat in a dose-dependent manner, with an IC_{50} value of 94 ± 1 nM. This experiment proves that sizzled acts directly on the catalytic domain of BMP-1, albeit that additional interactions with non-catalytic domains cannot be excluded.

To determine which domain of sizzled is responsible for BTP inhibition, we produced and purified its two separate domains. Residues Cys-115 in the Fz domain and Cys-159 in the NTR domain were also mutated to serines to avoid the presence of

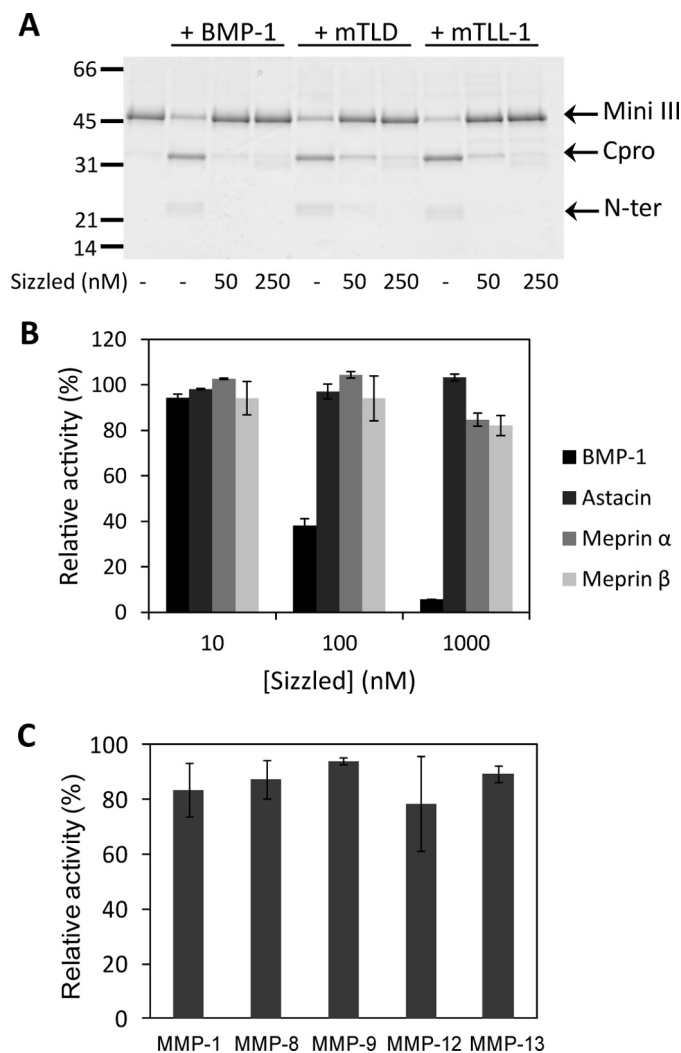


FIGURE 4. Sizzled is a specific inhibitor of BTPs. *A*, shown is the effect of sizzled on the activities of human BTPs. Mini-procollagen III (350 nM) was incubated at 37 $^{\circ}\text{C}$ with BMP-1 (25 nM), mTLD (25 nM), or mTLL-1 (25 nM) in the absence or presence of increasing sizzled concentrations (50 and 250 nM). Incubation times were calculated so that around 70% of mini-procollagen III was converted to C-propeptide and N-terminal cleavage product (50 min for BMP-1, 3 h for mTLD, and 5 h for mTLL-1). Analysis was by SDS-PAGE (4–20% acrylamide, reducing conditions) followed by staining with Coomassie Blue. *B*, shown is the effect of sizzled on the activities of human BMP-1 (21 nM), crayfish astacin (89 nM), human meprin α (1.9 nM), and human meprin β (0.8 nM). Each enzyme was incubated at 37 $^{\circ}\text{C}$ with the fluorogenic peptide Mca-YVADAPK(Dnp)-OH (20 μM) in the absence or presence of increasing sizzled concentrations (10, 100, and 1000 nM). Activities are expressed relative to activities in the absence of sizzled for each enzyme (means \pm range, $n = 2$). *C*, shown is the effect of sizzled on the activities of MMP-1 (0.51 nM), MMP-8 (0.85 nM), MMP-9 (0.11 nM), MMP-12 (3.1 nM), and MMP-13 (0.16 nM). Each enzyme was incubated at room temperature with the fluorogenic peptide Mca-PLGL(Dpa)AR-NH $_2$ (9 μM) in the absence or presence of 474 nM sizzled. Activities are expressed relative to the activities in the absence of sizzled for each enzyme (means \pm S.D., $n = 4$).

free cysteines (see below). As shown in Fig. 5B, the Fz domain alone was sufficient to inhibit the cleavage of the fluorogenic peptide by BMP-1. In contrast, when BMP-1 was incubated with the NTR domain, no visible inhibitory effect was observed. This is consistent with the observations of Lee *et al.* (20) on the selective binding of the Fz domain to *Xenopus* Xlr.

In summary, sizzled competitively inhibits the catalytic domain of BMP-1 by its Fz domain. Given the fact that the Fz domain of sFRP-1 and -2 is 50% identical to that of sizzled, it is

Control of BTP Activity by sFRPs

quite surprising that these sFRPs were unable to inhibit human BTPs. In an attempt to explain why sizzled is an inhibitor of BTPs whereas human sFRP-1 and mouse sFRP-2 are not, we next analyzed differences in sequences and secondary structures between these three proteins.

Sizzled Has an Interdomain Disulfide Bridge in Contrast to Mammalian sFRPs—One of the major differences between sFRPs and sizzled is found in their disulfide bonding patterns. The pattern of disulfide bonds in human sFRP-1 has previously been determined by Chong *et al.* (58); there are five disulfide bridges in the Fz domain and three in the NTR domain. Noteworthy, sizzled presents an additional cysteine residue (Cys-115) in its Fz domain and a missing cysteine residue in its NTR

domain, leaving Cys-159 unpaired (supplemental Fig. S4). Chong *et al.* (58) suggested that cysteines 115 and 159 might actually form an interdomain disulfide bridge. Another hypothesis would be that these two cysteines remain in their reduced state, thereby being potentially able to coordinate the active site zinc atom of BTPs or to react with a putative vicinal disulfide bridge located above the active site of BMP-1 (59).

To investigate these two possibilities, we cleaved sizzled with trypsin and analyzed the tryptic fragments by electrospray ionization-LC-MS. If one assumes that the disulfide bonds of sFRP-1 are conserved in sizzled and that sizzled contains an additional interdomain disulfide bridge between Cys-115 and Cys-159, tryptic digestion should lead to three major peptides (calculated masses 2155.5, 6046.1, and 9353.6 Da) (supplemental Fig. S4). These three peptides were indeed found by electrospray ionization LC-MS analysis (Table 1). Among them, the 9353.6-Da peptide includes five cysteine residues from the Fz domain and three from the NTR domain. To check that the interdomain disulfide bridge is formed between Cys-115 and Cys-159, we mutated these two residues to serines. This mutant as well as other mutants described below was characterized by MS (supplemental Table S2), and circular dichroism analysis showed that the mutations did not induce major changes in secondary structure elements (supplemental Fig. S5). Tryptic digestion of this mutant form of sizzled no longer generated the 9353.6-Da peptide but, rather, two shorter peptides (calculated masses 4205.8 and 5117.6 Da) corresponding to fragments from its NTR and Fz domains, respectively (Table 1). Altogether, these data indicate that sizzled contains an interdomain disulfide linkage between residues Cys-115 and Cys-159 that is not present in sFRP-1. However, using mini-procollagen III as a substrate, we found that mutation of these two cysteines had no effect on the ability of sizzled to inhibit BMP-1 (Table 2).

Analysis of Differences in Sequence between Sizzled and sFRP-1 and -2—We next sought to identify residues specific to sizzled that might be critical for BMP-1 inhibition. As previously reported (9, 20, 21) and as shown in Table 2, mutation of residue Asp-92 to asparagine dramatically decreased sizzled inhibitory activity. Sequence alignment of Fz domains from sizzled and human sFRPs (Fig. 1A) shows that this aspartate is conserved in sFRP-1, -2, and -5. Taking this into account, plausible explanations for the inability of sFRP-1 and -2 to inhibit BMP-1 are: 1) this aspartate may be hindered by other parts of the sFRP that prevent its access to BMP-1, and 2) there may be other residues specific to sizzled that are important for the inhibition.

To test the first hypothesis, we produced two constructs derived from sFRP-1, one without the NTR domain (sFRP-1-

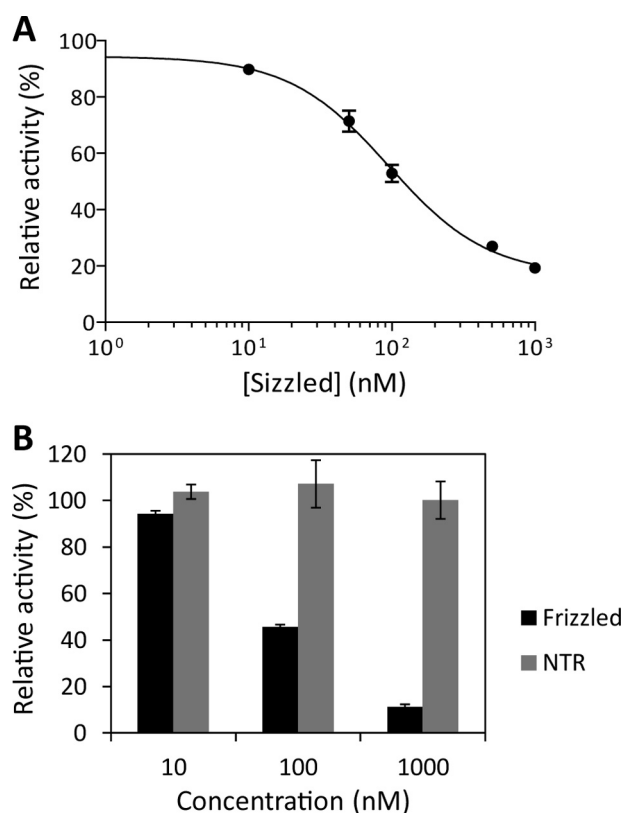


FIGURE 5. Sizzled inhibits the catalytic domain of BMP-1 by its Fz domain. A, shown is the effect of sizzled on the activity of the catalytic domain of BMP-1. The fluorogenic-quenched peptide Mca-YVADAPK(Dnp)-OH (20 μ M) was incubated at 37 °C with BMP-1cat (1 μ M) in the absence or presence of increasing concentrations of sizzled (10, 50, 100, 500, and 1000 nM). Error bars show S.D. ($n = 3$), and the line represents the fit obtained using GraphPad Prism 5. B, shown is the effect of Fz and NTR domains of sizzled on the activity of BMP-1. The fluorogenic-quenched peptide (20 μ M) was incubated at 37 °C with BMP-1 (36 nM) in the absence or presence of increasing concentrations of Fz or NTR domain (10, 100, and 1000 nM). Activities are expressed relative to activity in the absence of sizzled domains (means \pm S.D., $n = 5$).

TABLE 1

Electrospray ionization-LC-MS analyses of peptides obtained by tryptic digestion of sizzled and sizzled-C115S/C159S

Peptides	Sizzled		Sizzled-C115S/C159S	
	Calculated mass	Observed mass	Calculated mass	Observed mass
I (170Thr-Lys ¹⁸³)-(281Cys-Arg ²⁸⁵)	2155.5	2155.3	2155.5	2155.4
II (27Cys-Arg ⁴⁶)-(80Thr-Arg ⁹⁹)-(129Phe-Lys ¹⁴²)	6046.1	6046.4	6046.1	6046.8
III (63Ser-Arg ⁷⁹)-(100Ser-Arg ¹⁰⁶)-(107Asp-Arg ¹²⁸)-(150Glu-Lys ¹⁶⁹)-(219Thr-Lys ²³⁴)	9353.6	9354.6	(9321.4)	Not observed
IV (63Ser-Arg ⁷⁹)-(100Ser-Arg ¹⁰⁶)-(107Asp-Arg ¹²⁸)	5133.6	Not observed	5117.6	5117.9
V (150Glu-Lys ¹⁶⁹)-(219Thr-Lys ²³⁴)	4221.8	Not observed	4205.8	4206.5

TABLE 2

IC₅₀ values of sizzled, sFRP-1, and their mutants

Mini-procollagen III (340 nM) was incubated for 2 h at 37 °C with BMP-1 (17 nM) in the absence or presence of increasing concentrations of sizzled, sFRP-1, or their mutants. The products were analyzed by SDS-PAGE (4–20% acrylamide, reducing conditions) followed by staining with SYPRO Ruby (Sigma). Densitometric analysis of the gels was performed on a Storm 860 imager (GE Healthcare) and quantified using ImageQuant. Relative activity of BMP-1 as a function of inhibitor concentration was plotted. The curves were fitted using GraphPad Prism 5.

Sizzled mutants	IC ₅₀ values	sFRP1 mutants	IC ₅₀ values
Sizzled	<i>nm</i>	sFRP1	<i>nm</i>
Sizzled-C115S/C159S	15 ± 1	sFRP1-Fz	>1000
Sizzled-D92N	41 ± 4	sFRP1-ΔNterm	>300
Sizzled-F94A	>1000	sFRP1-R124T/P125F/Y127Q	>1000
Sizzled-Q96A	831 ± 28		>1000
Sizzled-S43A/E44A	52 ± 5		
Sizzled-K26A	415 ± 40		
	52 ± 3		

Fz) and one without the N-terminal extension (sFRP-1-ΔNterm). However, both these constructs proved to be unable to inhibit BMP-1 (Table 2). To explore the second hypothesis, we searched for residues that are conserved in sizzled but not in sFRP-1 and -2 and that are located in putative surface-exposed loops. For this purpose, we modeled the structure of the Fz domain of sizzled based on the known three-dimensional structures of the mouse sFRP-3 and frizzled-8 Fz domains (42) (Fig. 1, B and C). Using this model and the sequence alignment in Fig. 1A, we identified four promising target residues: Phe-94 (located in the same loop as Asp-92), Ser-43, Glu-44, and Lys-26 (located in nearby loops). Another target was Gln-96, in the same loop as Asp-92, which is also present in sFRP-2 but replaced by tyrosine in sFRP-1. All these residues were individually mutated to alanines, with the exception of Ser-43 and Glu-44, which were mutated as a pair.

Among residues that are located in the same loop as Asp-92, we found that the Q96A mutation only led to a small decrease of inhibition, whereas sizzled-F94A lost most of the inhibitory potency of sizzled with an IC₅₀ more than 50 times higher (Table 2). This suggests that several residues in the loop encompassing Asp-92 may play an important role in BMP-1 inhibition. To determine if the absence of sFRP-1 inhibiting activity is due only to its different amino acid sequence in this loop, we replaced it by that of sizzled. As shown in Table 2, this mutant of sFRP-1 (sFRP-1-R124T/P125F/Y127Q) remained unable to inhibit BMP-1.

This above result suggests that residues located in other putative loops might also play a role in BMP-1 inhibition. We found indeed that the double mutation S43A/E44A led to a severe drop in sizzled inhibiting activity, with an IC₅₀ value almost 30-fold higher than that of wild-type sizzled. As for the mutation K26A, this had no effect on the ability of sizzled to inhibit BMP-1 (Table 2). In conclusion, comparison of amino acid sequences of sizzled and sFRP-1 and -2 led us to identify new residues in sizzled involved in BMP-1 inhibition, both in the same loop as Asp-92 and in a nearby loop.

DISCUSSION

Until recently, BTPs had remained without any known endogenous specific inhibitor despite their implication in important processes during development and tissue repair. The

unexpected discovery that sizzled acts as a very potent inhibitor of BTPs during dorso-ventral patterning in *Xenopus* and zebrafish (24–26) raised the possibility that a similar regulatory mechanism might also be at work in mammals. Obvious candidates were mammalian sFRP-1–5, which have been extensively studied (9, 28, 29) but for which only one (sFRP-2) has emerged as a potential regulator of mammalian BTPs. However, the results are strongly divergent from one study to another and range from inhibition (28) to enhancement (9) or absence of any effect (29). The main basis of these studies was SDS-PAGE analysis of the effect of sFRP-2 on procollagen I processing by BMP-1 *in vitro*, with all the pitfalls inherent to gel-based quantification and limited demonstration of the reproducibility of the results.

For these reasons we compared the effects of three different mouse or human sFRPs (-1, -2, and -4) and of *Xenopus* sizzled on procollagen I processing using a quantitative assay. In these conditions we could unambiguously demonstrate that none of the tested mammalian sFRPs, not even sFRP-2, was capable of inhibiting or enhancing procollagen I processing, whereas sizzled led to a marked decrease of BMP-1 activity on this substrate. sFRP-2 was also tested at several concentrations ranging from 10 to 1000 nM and clearly appeared to have no significant effect on the procollagen C-proteinase activity of BMP-1, thus confirming the results obtained by von Marschall and Fisher (29). Two other precursor forms of fibrillar collagens, procollagen III and pN-collagen V, together with the cross-linking enzyme prolyl oxidase were also tested for the first time in the presence of sFRPs, and these experiments confirmed the absence of effect of the mammalian sFRPs on BMP-1. Finally, another quantitative assay using a quenched fluorescent peptide showed a similar behavior with no effect of sFRP-1, -2, and -4 and more than 80% inhibition in the presence of 100 nM sizzled. Altogether, these results question previous studies showing a direct effect of sFRP-2 on the procollagen C-proteinase activity of human BMP-1 and together with the results reported for chordin (9), dentin matrix protein-1, and dentin sialophosphoprotein (29) suggest that the absence of effect of mouse and human sFRPs can be extended to all BMP-1 activities.

It remains that interesting biological effects have been attributed to sFRP-2 and -3 in fibrotic diseases where excessive deposition of disorganized extracellular matrix, especially collagen, is observed. However, here again, controversial results have been obtained by the two groups who studied the effect of sFRP-2 in models of myocardial infarction, showing that the presence of sFRP-2 either aggravates or reduces the extent of fibrosis in relation to the level of collagen deposition (9, 28). We note that sFRPs seem to be extremely versatile molecules with biological effects that are highly context-dependent (19). For example, there is little certainty concerning their active forms in tissues (alone or in complex with other proteins), and two reports at least suggest that sFRP-1 and -3 could be present as monomers or form dimers through their Fz domains (42, 60). Thus, subtle differences in the state/conformation of sFRP-2 might explain some of the discrepancies between studies, and further insights into the structural properties of sFRPs would certainly help to settle some of the controversies. Moreover, in

Control of BTP Activity by sFRPs

both the above-mentioned studies, sFRP-2 seems to affect the total amount of procollagen I expressed by cells, complicating the analysis of the level of processing and suggesting that pathways unrelated to BMP-1 activity could also play roles in the infarcted heart. Indeed, sFRP-2 is known mainly as a Wnt antagonist, and as such, has been implicated in the control of cell apoptosis, proliferation, and differentiation (19). In agreement with this, mesenchymal stem cells overexpressing sFRP-2 seem to have enhanced ability to promote myocardial regeneration through increased proliferation and survival involving both Wnt and BMP signaling (61, 62). In addition, sFRP-2 has been shown to be up-regulated in hypertrophic scars resulting from abnormal healing of the skin (63), and sFRP-2 silencing in hypertrophic scar-derived fibroblasts promoted their apoptosis and led to down-regulation of α -smooth muscle actin, procollagen I, and procollagen III (64). In conclusion, although sFRP-2 clearly appears as an important player during healing of several organs, including heart and skin, its effects can also be mediated by the modulation of signaling pathways not directly related to BTPs. Noteworthy, although sFRP-3 seems to be without effect on the procollagen C-proteinase activity of BMP-1 (28), its therapeutic use for the prevention of hypertrophic scars has been patented (65).

Using surface plasmon resonance, we observed that sFRP-2 binds BMP-1, in agreement with previous studies (9, 28). Interestingly, sFRP-1 showed an even greater ability to interact with BMP-1, whereas sFRP-4 was unable to interact with the proteinase. Also, we found that sizzled lost its ability to interact with BMP-1 when the latter was immobilized on the sensor chip (data not shown), whereas sFRP-1 and -2 did not. This observation suggests that the three proteins do not share the same binding site on BMP-1 and may explain why they are not equally able to regulate BMP-1 activity. However, the potential role of the interaction between BMP-1 and sFRP-1 and -2 needs further clarification and should be carefully evaluated in the numerous biological contexts where they are co-expressed. These interactions could serve to control important aspects of the biological activity of BMP-1 or sFRPs, which are difficult to assess *in vitro*, like their diffusion or localization in specific micro-environments. Similar mechanisms have already been shown to regulate the activity of Wnt molecules, which can diffuse more efficiently in the presence of sFRPs (66).

Because the frizzled domain of sizzled displays around 50% identity and 77% similarity with the frizzled domains of human sFRP-1 and -2, the different behaviors of the three proteins must be explained by subtle modifications in sequences or structures of the three proteins. Careful examination of the amino acid composition and of a model of the frizzled domain of sizzled led us to identify three possible causes for the absence of activity of sFRP-1 and -2. The first was an additional cysteine residue in the Fz domain of sizzled which was unambiguously demonstrated in this study to be involved in an interdomain disulfide bridge and to have no effect on the inhibitory activity of sizzled. The second major difference between sizzled and sFRP-1 is a long N-terminal extension that is found before the Fz domain itself and is specific to sFRP-1 and, to a lesser extent, to sFRP-2. However, no appearance of sFRP-1 activity toward

BMP-1 was observed upon deletion of this N-terminal extension.

Much more conclusive was the comparison of the amino acids found in putative surface-exposed loops in sizzled and sFRP-1 or -2. As expected from previous reports (9, 20), the Asp-92 residue in sizzled, which is also present in sFRP-1 and -2, proved crucial for the inhibition of human BMP-1. This mutation is indeed responsible for the *ogon* mutation in zebrafish (25, 26), resulting in non-functional sizzled protein. This points to the loop surrounding Asp-92 as an important determinant of sizzled activity, as was confirmed by the decreased activity of the F94A mutant of sizzled. However, contributions from the non-conserved residues in the loop were not sufficient to explain the differences between sizzled and sFRP-1 as replacement of the three residues that were different in a region spanning six residues before and after Asp-92 did not confer inhibitory activity to sFRP-1. Further analysis revealed three other residues located in two different loops that are present in sizzled and absent in sFRP-1 and -2. Interestingly, residues Ser-43 and Glu-44 (also conserved as a pair in *Xenopus* crescent) but not Lys-26 seem to be involved in the interaction surface between sizzled and BMP-1, thereby delineating the first map of the binding site of BMP-1 on sizzled. As shown in Fig. 1, B and C, all the residues that were shown here to be important for this interaction are clustered in a defined region of the model of sizzled involving the loop preceding helix α 1 and the loop between helices α 3 and α 4. Most importantly also, we have shown that both conserved and non-conserved residues were required to allow the inhibitory complex with BMP-1 to form, explaining why sFRP-1 and -2 cannot form "productive" complexes with BMP-1. Interestingly, Ser-43 and Glu-44 in sizzled align with the KK motif in the short sequence ⁷⁴YKKM of sFRP-1, which has been shown to be necessary for Wnt3a antagonist activity (67), pointing to the important functional role played by this loop.

Our study also sheds light on how sizzled inhibits BMP-1. First of all, the absence of inhibition by the NTR domain of sizzled shows that the mechanism of BMP-1 inhibition by sizzled differs significantly from the inhibition of MMPs by TIMPs, which involves binding of the NTR domain of TIMPs in the catalytic pocket of MMPs (68). However, we demonstrate here for the first time that sizzled, like TIMPs, behaves as a tight binding inhibitor. Using the appropriate formalism for tight binding inhibitors, we showed that sizzled is a competitive inhibitor of BMP-1 with an inhibition constant as low as 1.5 ± 0.5 nM. In addition, inhibition by sizzled of the activity of the catalytic domain of BMP-1 confirms that sizzled mainly binds the catalytic domain of BMP-1, in agreement with the initial study by Lee *et al.* (20) on *Xenopus* tolloid Xlr that was then contradicted by a subsequent study involving human BMP-1 and mTLL-1 (9). An interesting consequence of this finding is that the conserved aspartate, which is crucial for sizzled activity (Asp-92), is probably located in the active site of BMP-1, but despite the strong preference of BTPs for aspartate in P1', this does not trigger cleavage of sizzled (nor of any of the tested sFRPs) by BMP-1. This observation is reminiscent of the mechanism used by crayfish astacin, the founder member of the astacin family, to achieve latency. Indeed, the three-dimensional

structure of the pro-astacin solved by Guevara *et al.* (69) reveals that the carboxyl group of the side chain of a conserved aspartic residue from the propeptide coordinates the catalytic zinc ion, thereby positioning the propeptide in a reverse orientation compared with the “normal” orientation seen with substrates. This precludes access of the substrate to the active site and activation of the water molecule required to achieve proteolysis. Because it is very likely that the equivalent aspartate in BMP-1 and other BTPs plays a similar role (69), we can also speculate that Asp-92 in sizzled could coordinate the zinc and thereby prevent its cleavage by the protease. Also, the three-dimensional structure of the catalytic domain of BMP-1 (59) revealed the presence of an arginine residue (Arg-176 corresponding to Arg-302 in the full-length BMP-1) in the S1' pocket that would be well positioned to interact with Glu-44 in sizzled and to further stabilize the enzyme-inhibitor complex.

Another interesting feature of sizzled that was also demonstrated here is its high specificity for BTPs. Although all three BTPs tested (BMP-1, mTLD, and mTLL-1) were inhibited by sizzled, other members of the astacin family, such as astacin itself and human meprins α and β (that demonstrate the same preference for acidic residues in P1' as BTPs (70)), were not inhibited or enhanced by sizzled. Similarly, sizzled had no effect on five well characterized MMPs (-1, -8, -9, -12, and -13) and, in contrast to other sFRPs including crescent (27), also seems unable to modulate Wnt signaling (23–25). Consequently, it seems that thanks to its potency and specificity, sizzled could be an appropriate tool to study the biological roles of BTPs in complex systems and potentially to derive novel classes of BTP inhibitors that could be used to prevent fibrotic disorders.

Acknowledgments—We thank E. De Robertis, E. Canty, and A. Sieron for providing plasmids and E. Pêcheur for technical assistance with the TECAN fluorimeter. We also thank A. Chaboud (Plateau Production et Analyse des Protéines; UMS3444) for technical support and I. Zanella-Cleon (Centre Commun de Micronalyse des Protéines; UMS3444) for mass spectrometry analyses.

REFERENCES

- Muir, A., and Greenspan, D. S. (2011) Metalloproteinases in *Drosophila* to humans that are central players in developmental processes. *J. Biol. Chem.* **286**, 41905–41911
- Takahara, K., Lyons, G. E., and Greenspan, D. S. (1994) Bone morphogenetic protein-1 and a mammalian tolloid homologue (mTld) are encoded by alternatively spliced transcripts which are differentially expressed in some tissues. *J. Biol. Chem.* **269**, 32572–32578
- Scott, I. C., Blitz, I. L., Pappano, W. N., Imamura, Y., Clark, T. G., Steiglitz, B. M., Thomas, C. L., Maas, S. A., Takahara, K., Cho, K. W., and Greenspan, D. S. (1999) Mammalian BMP-1/Tolloid-related metalloproteinases, including novel family member mammalian Tolloid-like 2, have differential enzymatic activities and distributions of expression relevant to patterning and skeletogenesis. *Dev. Biol.* **213**, 283–300
- Takahara, K., Brevard, R., Hoffman, G. G., Suzuki, N., and Greenspan, D. S. (1996) Characterization of a novel gene product (mammalian tolloid-like) with high sequence similarity to mammalian tolloid/bone morphogenetic protein-1. *Genomics* **34**, 157–165
- Leighton, M., and Kadler, K. E. (2003) Paired basic/Furin-like proprotein convertase cleavage of Pro-BMP-1 in the trans-Golgi network. *J. Biol. Chem.* **278**, 18478–18484
- Bond, J. S., and Beynon, R. J. (1995) The astacin family of metalloendopeptidases. *Protein Sci.* **4**, 1247–1261
- Ge, G., and Greenspan, D. S. (2006) Developmental roles of the BMP1/TLD metalloproteinases. *Birth Defects Res. C Embryo Today* **78**, 47–68
- Grgurevic, I., Macek, B., Healy, D. R., Brault, A. L., Erjavec, I., Cipic, A., Grgurevic, I., Rogic, D., Galesic, K., Brkljacic, J., Stern-Padovan, R., Paralkar, V. M., and Vukicevic, S. (2011) Circulating bone morphogenetic protein 1–3 isoform increases renal fibrosis. *J. Am. Soc. Nephrol.* **22**, 681–692
- Kobayashi, K., Luo, M., Zhang, Y., Wilkes, D. C., Ge, G., Grieskamp, T., Yamada, C., Liu, T. C., Huang, G., Basson, C. T., Kispert, A., Greenspan, D. S., and Sato, T. N. (2009) Secreted Frizzled-related protein 2 is a pro-collagen C proteinase enhancer with a role in fibrosis associated with myocardial infarction. *Nat. Cell Biol.* **11**, 46–55
- Moali, C., and Hulmes, D. J. (2012) in *Extracellular Matrix: Pathobiology and Signaling* (Karamanos, M., ed) pp. 539–561, De Gruyter, Berlin
- Adar, R., Kessler, E., and Goldberg, B. (1986) Evidence for a protein that enhances the activity of type I procollagen C-proteinase. *Coll. Relat. Res.* **6**, 267–277
- Moali, C., Font, B., Ruggiero, F., Eichenberger, D., Rousselle, P., François, V., Oldberg, A., Bruckner-Tuderman, L., and Hulmes, D. J. (2005) Substrate-specific modulation of a multisubstrate proteinase. C-terminal processing of fibrillar procollagens is the only BMP-1-dependent activity to be enhanced by PCPE-1. *J. Biol. Chem.* **280**, 24188–24194
- Steiglitz, B. M., Keene, D. R., and Greenspan, D. S. (2002) PCOLCE2 encodes a functional procollagen C-proteinase enhancer (PCPE2) that is a collagen-binding protein differing in distribution of expression and post-translational modification from the previously described PCPE1. *J. Biol. Chem.* **277**, 49820–49830
- Inomata, H., Haraguchi, T., and Sasai, Y. (2008) Robust stability of the embryonic axial pattern requires a secreted scaffold for chordin degradation. *Cell* **134**, 854–865
- Scott, I. C., Blitz, I. L., Pappano, W. N., Maas, S. A., Cho, K. W., and Greenspan, D. S. (2001) Homologues of Twisted gastrulation are extracellular cofactors in antagonism of BMP signaling. *Nature* **410**, 475–478
- Maruhashi, T., Kii, I., Saito, M., and Kudo, A. (2010) Interaction between periostin and BMP-1 promotes proteolytic activation of lysyl oxidase. *J. Biol. Chem.* **285**, 13294–13303
- Lee, H. X., Mendes, F. A., Plouhinec, J. L., and De Robertis, E. M. (2009) Enzymatic regulation of pattern. BMP4 binds CUB domains of Tolloids and inhibits proteinase activity. *Genes Dev.* **23**, 2551–2562
- Jasuja, R., Ge, G., Voss, N. G., Lyman-Gingerich, J., Branam, A. M., Pelegri, F. J., and Greenspan, D. S. (2007) Bone morphogenetic protein 1 prodomain specifically binds and regulates signaling by bone morphogenetic proteins 2 and 4. *J. Biol. Chem.* **282**, 9053–9062
- Bovolenta, P., Esteve, P., Ruiz, J. M., Cisneros, E., and Lopez-Rios, J. (2008) Beyond Wnt inhibition. New functions of secreted Frizzled-related proteins in development and disease. *J. Cell Sci.* **121**, 737–746
- Lee, H. X., Ambrosio, A. L., Reversade, B., and De Robertis, E. M. (2006) Embryonic dorsal-ventral signaling. Secreted frizzled-related proteins as inhibitors of tolloid proteinases. *Cell* **124**, 147–159
- Muraoka, O., Shimizu, T., Yabe, T., Nojima, H., Bae, Y. K., Hashimoto, H., and Hibi, M. (2006) Sizzled controls dorso-ventral polarity by repressing cleavage of the Chordin protein. *Nat. Cell Biol.* **8**, 329–338
- Salic, A. N., Kroll, K. L., Evans, L. M., and Kirschner, M. W. (1997) Sizzled. A secreted Xwnt8 antagonist expressed in the ventral marginal zone of *Xenopus* embryos. *Development* **124**, 4739–4748
- Bradley, L., Sun, B., Collins-Racie, L., LaVallie, E., McCoy, J., and Sive, H. (2000) Different activities of the frizzled-related proteins frzb2 and sizzled2 during *Xenopus* anteroposterior patterning. *Dev. Biol.* **227**, 118–132
- Collavin, L., and Kirschner, M. W. (2003) The secreted Frizzled-related protein Sizzled functions as a negative feedback regulator of extreme ventral mesoderm. *Development* **130**, 805–816
- Yabe, T., Shimizu, T., Muraoka, O., Bae, Y. K., Hirata, T., Nojima, H., Kawakami, A., Hirano, T., and Hibi, M. (2003) Ogon/Secreted Frizzled functions as a negative feedback regulator of Bmp signaling. *Development* **130**, 2705–2716
- Martyn, U., and Schulte-Merker, S. (2003) The ventralized ogon mutant phenotype is caused by a mutation in the zebrafish homologue of Sizzled, a secreted Frizzled-related protein. *Dev. Biol.* **260**, 58–67

27. Ploper, D., Lee, H. X., and De Robertis, E. M. (2011) Dorsal-ventral patterning. Crescent is a dorsally secreted Frizzled-related protein that competitively inhibits Tollid proteases. *Dev. Biol.* **352**, 317–328
28. He, W., Zhang, L., Ni, A., Zhang, Z., Mirotosu, M., Mao, L., Pratt, R. E., and Dzau, V. J. (2010) Exogenously administered secreted frizzled-related protein 2 (Sfrp2) reduces fibrosis and improves cardiac function in a rat model of myocardial infarction. *Proc. Natl. Acad. Sci. U.S.A.* **107**, 21110–21115
29. von Marschall, Z., and Fisher, L. W. (2010) Dentin sialophosphoprotein (DSPP) is cleaved into its two natural dentin matrix products by three isoforms of bone morphogenetic protein-1 (BMP1). *Matrix Biol.* **29**, 295–303
30. Martin, R., Farjanel, J., Eichenberger, D., Giraud-Guille, M. M., and Hulmes, D. J. (2000) Large scale production of procollagen I from chick embryo tendon fibroblasts. *Anal. Biochem.* **277**, 276–278
31. Fichard, A., Tillet, E., Delacoux, F., Garrone, R., and Ruggiero, F. (1997) Human recombinant $\alpha 1(V)$ collagen chain. Homotrimeric assembly and subsequent processing. *J. Biol. Chem.* **272**, 30083–30087
32. Blanc, G., Font, B., Eichenberger, D., Moreau, C., Ricard-Blum, S., Hulmes, D. J., and Moali, C. (2007) Insights into how CUB domains can exert specific functions while sharing a common-fold. Conserved and specific features of the CUB1 domain contribute to the molecular basis of procollagen C-proteinase enhancer-1 activity. *J. Biol. Chem.* **282**, 16924–16933
33. Berry, R., Jowitz, T. A., Garrigue-Antar, L., Kadler, K. E., and Baldock, C. (2010) Structural and functional evidence for a substrate exclusion mechanism in mammalian tollid like-1 (TLL-1) proteinase. *FEBS Lett.* **584**, 657–661
34. Becker-Pauly, C., Höwel, M., Walker, T., Vlad, A., Aufenvenne, K., Oji, V., Lottaz, D., Sterchi, E. E., Debela, M., Magdolen, V., Traupe, H., and Stöcker, W. (2007) The α and β subunits of the metalloproteinase meprin are expressed in separate layers of human epidermis, revealing different functions in keratinocyte proliferation and differentiation. *J. Invest. Dermatol.* **127**, 1115–1125
35. Becker, C., Kruse, M. N., Sloty, K. A., Köhler, D., Harris, J. R., Rösmann, S., Sterchi, E. E., and Stöcker, W. (2003) Differences in the activation mechanism between the α and β subunits of human meprin. *Biol. Chem.* **384**, 825–831
36. Wermter, C., Höwel, M., Hintze, V., Bombosch, B., Aufenvenne, K., Yiallourous, I., and Stöcker, W. (2007) The protease domain of procollagen C-proteinase (BMP1) lacks substrate selectivity, which is conferred by non-proteolytic domains. *Biol. Chem.* **388**, 513–521
37. Reyda, S., Jacob, E., Zwilling, R., and Stöcker, W. (1999) cDNA cloning, bacterial expression, *in vitro* renaturation, and affinity purification of the zinc endopeptidase astacin. *Biochem. J.* **344**, 851–857
38. Yiallourous, I., Grosse Berkhoff, E., and Stöcker, W. (2000) The roles of Glu-93 and Tyr-149 in astacin-like zinc peptidases. *FEBS Lett.* **484**, 224–228
39. Dabert-Gay, A. S., Czarny, B., Devel, L., Beau, F., Lajeunesse, E., Bregant, S., Thai, R., Yiotakis, A., and Dive, V. (2008) Molecular determinants of matrix metalloproteinase-12 covalent modification by a photoaffinity probe. Insights into activity-based probe development and conformational variability of matrix metalloproteinases. *J. Biol. Chem.* **283**, 31058–31067
40. Tochowicz, A., Maskos, K., Huber, R., Oltenfreiter, R., Dive, V., Yiotakis, A., Zanda, M., Pourmotabbed, T., Bode, W., and Goettig, P. (2007) Crystal structures of MMP-9 complexes with five inhibitors. Contribution of the flexible Arg-424 side chain to selectivity. *J. Mol. Biol.* **371**, 989–1006
41. Kronenberg, D., Bruns, B. C., Moali, C., Vadon-Le Goff, S., Sterchi, E. E., Traupe, H., Böhm, M., Hulmes, D. J., Stöcker, W., and Becker-Pauly, C. (2010) Processing of procollagen III by meprins. New players in extracellular matrix assembly? *J. Invest. Dermatol.* **130**, 2727–2735
42. Dann, C. E., Hsieh, J. C., Rattner, A., Sharma, D., Nathans, J., and Leahy, D. J. (2001) Insights into Wnt binding and signalling from the structures of two Frizzled cysteine-rich domains. *Nature* **412**, 86–90
43. Sali, A., and Blundell, T. L. (1993) Comparative protein modeling by satisfaction of spatial restraints. *J. Mol. Biol.* **234**, 779–815
44. Chen, V. B., Arendall, W. B., 3rd, Headd, J. J., Keedy, D. A., Immormino, R. M., Kapral, G. J., Murray, L. W., Richardson, J. S., and Richardson, D. C. (2010) MolProbity. All-atom structure validation for macromolecular crystallography. *Acta Crystallogr. D. Biol. Crystallogr.* **66**, 12–21
45. Petropoulou, V., Garrigue-Antar, L., and Kadler, K. E. (2005) Identification of the minimal domain structure of bone morphogenetic protein-1 (BMP-1) for chordinase activity. Chordinase activity is not enhanced by procollagen C-proteinase enhancer-1 (PCPE-1). *J. Biol. Chem.* **280**, 22616–22623
46. Canty, E. G., and Kadler, K. E. (2005) Procollagen trafficking, processing and fibrillogenesis. *J. Cell Sci.* **118**, 1341–1353
47. Hojima, Y., van der Rest, M., and Prockop, D. J. (1985) Type I procollagen carboxyl-terminal proteinase from chick embryo tendons. Purification and characterization. *J. Biol. Chem.* **260**, 15996–16003
48. Wawrzak, D., Métioui, M., Willems, E., Hendrickx, M., de Genst, E., and Leyns, L. (2007) Wnt3a binds to several sFRPs in the nanomolar range. *Biochem. Biophys. Res. Commun.* **357**, 1119–1123
49. Gopalakrishnan, B., Wang, W. M., and Greenspan, D. S. (2004) Biosynthetic processing of the Pro- $\alpha 1(V)$ Pro- $\alpha 2(V)$ Pro- $\alpha 3(V)$ procollagen heterotrimer. *J. Biol. Chem.* **279**, 30904–30912
50. Imamura, Y., Steigltz, B. M., and Greenspan, D. S. (1998) Bone morphogenetic protein-1 processes the NH₂-terminal propeptide, and a furin-like proprotein convertase processes the COOH-terminal propeptide of pro- $\alpha 1(V)$ collagen. *J. Biol. Chem.* **273**, 27511–27517
51. Kessler, E., Fichard, A., Chanut-Delalande, H., Brusel, M., and Ruggiero, F. (2001) Bone morphogenetic protein-1 (BMP-1) mediates C-terminal processing of procollagen V homotrimer. *J. Biol. Chem.* **276**, 27051–27057
52. Unsöld, C., Pappano, W. N., Imamura, Y., Steigltz, B. M., and Greenspan, D. S. (2002) Biosynthetic processing of the pro- $\alpha 1(V)$ 2pro- $\alpha 2(V)$ collagen heterotrimer by bone morphogenetic protein-1 and furin-like proprotein convertases. *J. Biol. Chem.* **277**, 5596–5602
53. Cronshaw, A. D., Fothergill-Gilmore, L. A., and Hulmes, D. J. (1995) The proteolytic processing site of the precursor of lysyl oxidase. *Biochem. J.* **306**, 279–284
54. Enari, M., Talanian, R. V., Wong, W. W., and Nagata, S. (1996) Sequential activation of ICE-like and CPP32-like proteases during Fas-mediated apoptosis. *Nature* **380**, 723–726
55. Sterchi, E. E., Stöcker, W., and Bond, J. S. (2008) Meprins, membrane-bound and -secreted astacin metalloproteinases. *Mol. Aspects Med.* **29**, 309–328
56. Copeland, R. A. (2000) in *Enzymes: A practical introduction to structure, mechanism, and data analysis* (Copeland, R. A., ed) pp. 305–317, John Wiley and Sons, New York
57. Morrison, J. F. (1969) Kinetics of the reversible inhibition of enzyme-catalyzed reactions by tight binding inhibitors. *Biochim. Biophys. Acta* **185**, 269–286
58. Chong, J. M., Uren, A., Rubin, J. S., and Speicher, D. W. (2002) Disulfide bond assignments of secreted Frizzled-related protein-1 provide insights about Frizzled homology and netrin modules. *J. Biol. Chem.* **277**, 5134–5144
59. Mac Sweeney, A., Gil-Parrado, S., Vinzenz, D., Bernardi, A., Hein, A., Bodendorf, U., Erbel, P., Logel, C., and Gerhartz, B. (2008) Structural basis for the substrate specificity of bone morphogenetic protein 1/tollid-like metalloproteinases. *J. Mol. Biol.* **384**, 228–239
60. Bafico, A., Gazit, A., Pramila, T., Finch, P. W., Yaniv, A., and Aaronson, S. A. (1999) Interaction of frizzled-related protein (FRP) with Wnt ligands and the frizzled receptor suggests alternative mechanisms for FRP inhibition of Wnt signaling. *J. Biol. Chem.* **274**, 16180–16187
61. Alfaro, M. P., Pagni, M., Vincent, A., Atkinson, J., Hill, M. F., Cates, J., Davidson, J. M., Rottman, J., Lee, E., and Young, P. P. (2008) The Wnt modulator sFRP2 enhances mesenchymal stem cell engraftment, granulation tissue formation, and myocardial repair. *Proc. Natl. Acad. Sci. U.S.A.* **105**, 18366–18371
62. Alfaro, M. P., Vincent, A., Saraswati, S., Thorne, C. A., Hong, C. C., Lee, E., and Young, P. P. (2010) sFRP2 suppression of bone morphogenetic protein (BMP) and Wnt signaling mediates mesenchymal stem cell (MSC) self-renewal promoting engraftment and myocardial repair. *J. Biol. Chem.* **285**, 35645–35653
63. Chen, W., Fu, X., Sun, X., Sun, T., Zhao, Z., and Sheng, Z. (2003) Analysis of differentially expressed genes in keloids and normal skin with cDNA

- microarray. *J. Surg. Res.* **113**, 208–216
64. Sun, Z., Li, S., Cao, C., Wu, J., Ma, B., and Tran, V. (2011) shRNA targeting SFRP2 promotes the apoptosis of hypertrophic scar fibroblast. *Mol. Cell Biochem.* **352**, 25–33
65. Ferguson, M. W. J., Lavery, H., Occeleston, N., O’Kane, S., and Nield, K. (2008) International Patent WO 2008/125869
66. Mii, Y., and Taira, M. (2009) Secreted Frizzled-related proteins enhance the diffusion of Wnt ligands and expand their signalling range. *Development* **136**, 4083–4088
67. Bhat, R. A., Stauffer, B., Komm, B. S., and Bodine, P. V. (2007) Structure-function analysis of secreted frizzled-related protein-1 for its Wnt antagonist function. *J. Cell. Biochem.* **102**, 1519–1528
68. Brew, K., Dinakarandian, D., and Nagase, H. (2000) Tissue inhibitors of metalloproteinases. Evolution, structure, and function. *Biochim. Biophys. Acta* **1477**, 267–283
69. Guevara, T., Yiallourous, I., Kappelhoff, R., Bissdorf, S., Stöcker, W., and Gomis-Rüth, F. X. (2010) Proenzyme structure and activation of astacin metallopeptidase. *J. Biol. Chem.* **285**, 13958–13965
70. Becker-Pauly, C., Barre, O., Schilling, O., Uf dem, K. U., Ohler, A., Broder, C., Schutte, A., Kappelhoff, R., Stöcker, W., and Overall, C. M. (2011) Proteomic analyses reveal an acidic prime side specificity for the astacin metalloprotease family reflected by physiological substrates. *Mol. Cell. Proteomics* doi: M111.009233
71. Larkin, M. A., Blackshields, G., Brown, N. P., Chenna, R., McGettigan, P. A., McWilliam, H., Valentin, F., Wallace, I. M., Wilm, A., Lopez, R., Thompson, J. D., Gibson, T. J., and Higgins, D. G. (2007) Clustal W and Clustal X Version 2.0. *Bioinformatics* **23**, 2947–2948
72. Gouet, P., Courcelle, E., Stuart, D. I., and Métoz, F. (1999) ESPript. Analysis of multiple sequence alignments in PostScript. *Bioinformatics.* **15**, 305–308

Enzymology:

Sizzled Is Unique among Secreted Frizzled-related Proteins for Its Ability to Specifically Inhibit Bone Morphogenetic Protein-1 (BMP-1)/Tolloid-like Proteinases

ENZYMOLOGY

Cécile Bijakowski, Sandrine Vadon-Le Goff, Frédéric Delolme, Jean-Marie Bourhis, Pascaline Lécorché, Florence Ruggiero, Christoph Becker-Pauly, Irene Yiallourous, Walter Stöcker, Vincent Dive, David J. S. Hulmes and Catherine Moali

J. Biol. Chem. 2012, 287:33581-33593.

doi: 10.1074/jbc.M112.380816 originally published online July 23, 2012

Access the most updated version of this article at doi: [10.1074/jbc.M112.380816](https://doi.org/10.1074/jbc.M112.380816)

Find articles, minireviews, Reflections and Classics on similar topics on the [JBC Affinity Sites](http://www.jbc.org/).

Alerts:

- [When this article is cited](#)
- [When a correction for this article is posted](#)

[Click here](#) to choose from all of JBC's e-mail alerts

Supplemental material:

<http://www.jbc.org/content/suppl/2012/07/23/M112.380816.DC1.html>

This article cites 69 references, 34 of which can be accessed free at <http://www.jbc.org/content/287/40/33581.full.html#ref-list-1>